Preprints of the 10th IFAC International Symposium on Dynamics and Control of Process Systems
The International Federation of Automatic Control
December 18-20, 2013. Mumbai, India

State and Parameter Estimation for a Grinding Mill Circuit from Operational Input-Output Data

Johan D. le Roux * **Ian K. Craig** * **Radhakant Padhi** **

* *Department of Electrical, Electronic, and Computer Engineering, University of Pretoria, Pretoria, South Africa.*
** *Visiting Professor, University of Pretoria, Pretoria, South Africa*

Abstract: The states and unknown parameters of a simplified non-linear grinding mill circuit model for process control was estimated from real plant data by means of an Extended Kalman Filter. The output of the model as calculated from the states and parameters estimated by the Extended Kalman Filter closely follow the actual output of the plant. The continuous estimate of states and parameters from plant data allows for the continuous update of a process model used for process control. This limits model-plant mismatch which deteriorates controller performance.

Keywords: comminution, estimation, grinding, kalman filter

1. INTRODUCTION

A grinding mill circuit is generally difficult to control because of strong coupling between variables, large time delays, uncontrollable disturbances, the variation of parameters over time, the non-linearities in the process and instrumentation inadequacies. Though model predictive controllers can successfully control a grinding mill circuit, the performance of the controller depends on the quality of the plant model that is available (Chen et al., 2007). Model-plant mismatch, which deteriorates controller performance, occurs when unknown parameters and unmeasurable states in a grinding mill circuit are estimated incorrectly. Because of the time-varying nature of the process, the process model needs to be updated continuously to minimize the effect of model-plant mismatch on controller performance (Olivier et al., 2012).

This study aims to estimate the states and unknown parameters of a non-linear grinding mill circuit model developed for process control purposes by means of an Extended Kalman Filter (EKF). Real plant data is used to estimate the states and unknown parameters of the model.

2. PROCESS DESCRIPTION

The three main elements of the single-stage closed grinding mill circuit shown in Fig. 1 are the mill, the sump and the classification screen. The circuit variables are described in Table 1. The mill receives four streams: oversize from the screen, mined ore (MFS), water (MIW) and additional steel balls (MFB) to assist with the breakage of ore. The mill rotates and lifts the material in the mill. At a certain height the material falls back on itself. This causes the ore to break either through impact, abrasion or attrition. The ground ore in the mill mixes with the water to create a slurry. The volume of charge in the mill is represented by $LOAD$. The slurry in the mill is then discharged to the sump either by overflow or through a discharge screen. In the case of the discharge screen, the particle size of the discharged slurry from the mill is limited by the aperture size of the screen. The volume of slurry in the sump is represented by $SVOL$. The slurry in the sump is diluted with water (SFW) before it is pumped to the classification screen. Spillage water is also added to the sump, but is not necessarily a manipulated variable. The outflow from the pump is the classifier feed flow-rate CFF and the density of the classifier feed is CFD. The slurry flow across the classification screen can either pass through the apertures in the screen as undersize material or over the apertures in the screen to be discharged from the screen as oversize material. The process of classification is assisted by the addition of water to the screen (CWA). The oversize flow of slurry is returned to the mill for further grinding. The undersize flow of slurry contains the final product (PSE) that is passed to a downstream process (Napier-Munn et al., 1999; Coetzee et al., 2010).

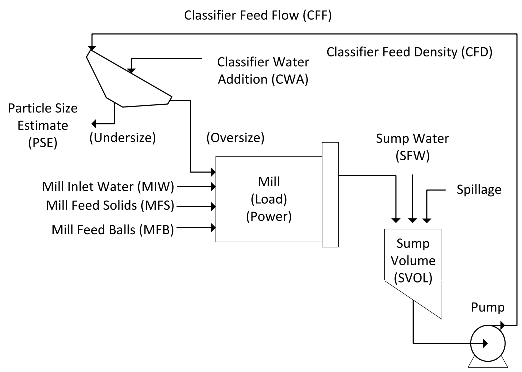

Fig. 1. A single-stage grinding mill circuit closed with a classification screen.

Table 1. Description of circuit variables

Manipulated Variables	
MIW	flow-rate of water to the mill [m^3/h]
MFS	feed-rate of ore to the mill [t/h]
MFB	feed-rate of steel balls to the mill [t/h]
SFW	flow-rate of water to the sump [m^3/h]
CFF	flow-rate of slurry to the classifier [m^3/h]
CWA	flow-rate of water to the classifier [m^3/h]
Controlled Variables	
$LOAD$	volume of charge within the mill [m^3]
$SVOL$	volume of slurry in sump [m^3]
CFD	classifier feed density [t/m^3]
PSE	product particle size estimate [%]

Table 2. Description of subscripts

Subscript	Description
$X_{\Delta -}$	f-feeder; m-mill; s-sump; c-cyclone
$X_{-\Delta}$	w-water; s-solids; c-coarse; f-fines; r-rocks; b-balls
$V_{--\Delta}$	i-inflow; o-outflow; os-oversize; us-undersize

3. MODEL DESCRIPTION

The model used to describe the circuit in Fig. 1 consists of four modules: a feeder, a semi-autogenous mill with an end-discharge screen, a sump and a classification screen. All the modules, except the feeder, can be seen in Fig. 1.

The feeder, mill and sump modules can be described by the reduced complexity non-linear model found in le Roux et al. (2013), of which a brief description is given below. The approach in the derivation of the model was to use as few fitted parameters as possible while making the model produce responses that are reasonably accurate and in the right direction. The sizing performance of the classification screen is modelled by an efficiency curve.

The model uses five states to represent the constituents of charge in the milling circuit. The states are rocks, solids, fines, balls and water. Rocks are ore too large to be discharged from the mill, whereas solids are ore that can be discharged from the mill. The solids consist of the sum of fine and coarse ore, where fine ore is smaller than the product specification size and coarse ore is larger than the product specification size. Balls and rocks are only found in the mill, as they are too large to pass through the apertures in the end-discharge screen.

Each of the four modules and their mathematical descriptions are shown below. For the equations, V denotes a flow-rate in m^3/h and X denotes the states of the model as volumes in m^3. Table 2 provides a description of the subscripts for V and X. The first subscript indicates the module considered, the second subscript specifies which of the five states are considered and in the case of flow-rates the final subscript shows if it is an inflow, outflow, oversize or undersize flow. The nomenclature for the model is shown in Table 3.

3.1 Feeder Module

The feeder module divides the ore fed to the mill into various streams. Each stream represents the flow-rate of one of the five states out of the feeder module into the mill module: water (V_{fwo}), solids (V_{fso}), fines (V_{ffo}), rocks (V_{fro}) and balls (V_{fbo}). The flow-rates are defined as:

Table 3. Feeder, mill and screen parameters

Feeder and Mill Parameters	
α_f	Fraction fines in the ore
α_r	Fraction rock in the ore
α_P	Fractional power reduction per fractional reduction from maximum mill speed
α_{ϕ_f}	Fractional change in kW/fines produced per change in fractional filling of mill
α_{speed}	Fraction of critical mill speed
δ_{P_s}	Power-change parameter for fraction solids in the mill
δ_{P_v}	Power-change parameter for volume of mill filled
D_B	Density of steel balls [t/m^3]
D_S	Density of feed ore [t/m^3]
ε_{sv}	Max fraction solids by slurry volume at 0 slurry flow
ϕ_b	Steel abrasion factor [kWh/t]
ϕ_f	Power needed per tonne of fines produced [kWh/t]
ϕ_r	Rock abrasion factor [kWh/t]
$\varphi_{P_{max}}$	Rheology factor for max mill power draw
P_{max}	Maximum mill motor power draw [kW]
v_{mill}	Mill volume [m^3]
$v_{P_{max}}$	Fraction of mill volume filled for max power draw
V_V	Volumetric flow per flowing volume driving force [h^{-1}]
χ_P	Cross-term for maximum power draw
Screen Parameters	
D_1	Split of solids to oversize
D_2	Fitting constant for product size estimate
Time Delays	
T_{sc}	Time delay between sump and classifier [s]
T_{cm}	Time delay between classifier and mill [s]

$$V_{fwo} = MIW \tag{1}$$
$$V_{fso} = MFS(1-\alpha_r)/D_S \tag{2}$$
$$V_{ffo} = MFS\alpha_f/D_S \tag{3}$$
$$V_{fro} = MFS\alpha_r/D_S \tag{4}$$
$$V_{fbo} = MFB/D_B \tag{5}$$

3.2 Mill Module

The population volume balance of the hold-up of water (X_{mw}), solids (X_{ms}), fines (X_{mf}), rocks (X_{mr}) and balls (X_{mb}) in the mill are defined in terms of the inflow and outflow of each state:

$$\dot{X}_{mw} = V_{fwo} + V_{cwos} - V_{mwo} \tag{6}$$
$$\dot{X}_{ms} = V_{fso} + V_{csos} - V_{mso} + RC \tag{7}$$
$$\dot{X}_{mf} = V_{ffo} + V_{cfos} - V_{mfo} + FP \tag{8}$$
$$\dot{X}_{mr} = V_{fro} - RC \tag{9}$$
$$\dot{X}_{mb} = V_{fbo} - BC \tag{10}$$

where RC, BC and FP refer to rock consumption, ball consumption and fines production respectively. These three breakage functions are described in eqs. (16), (17) and (18) respectively.

The mill outlet flow-rates for water (V_{mwo}), solids (V_{mso}), fines (V_{mfo}), rocks (V_{mro}) and balls (V_{mbo}) are defined as:

$$V_{mwo} = V_V\varphi X_{mw}^2/\left(X_{ms}+X_{mw}\right) \tag{11}$$
$$V_{mso} = V_V\varphi X_{mw}X_{ms}/\left(X_{ms}+X_{mw}\right) \tag{12}$$
$$V_{mfo} = V_V\varphi X_{mw}X_{mf}/\left(X_{ms}+X_{mw}\right) \tag{13}$$

where $V_{mro} = 0$ and $V_{mbo} = 0$ because balls and rocks do not pass through the mill's end-discharge screen.

The model adds the effect of the rheology of the slurry on the milling performance by means of the empirically defined rheology factor $\varphi = \left\{\max\left[0, 1-\left(\frac{\varepsilon_{sv}-1}{\varepsilon_{sv}}\right)\frac{X_{ms}}{X_{mw}}\right]\right\}^{\frac{1}{2}}$.

The mill-power draw is defined as:

$$P_{mill} = P_{max}(\alpha_{speed})^{\alpha_P} \\ \{1 - \delta_{Pv} Z_x^2 - 2\chi_P \delta_{Pv} \delta_{Ps} Z_x Z_r - \delta_{Ps} Z_r^2\} \tag{14}$$

where the effect of the volume of the mill filled on power consumption is defined as $Z_x = \frac{LOAD}{v_{mill} v_{P_{max}}} - 1$ and the effect of the slurry rheology on power consumption is defined as $Z_r = \frac{\varphi}{\varphi_{P_{max}}} - 1$. The total volume of the mill filled is given by:

$$LOAD = X_{mw} + X_{mr} + X_{ms} + X_{mb} \tag{15}$$

As the ore grinds in the mill it results in the consumption of rocks and balls over time, as well as the production of fines. The definition for rock consumption is:

$$RC = \frac{P_{mill}\varphi}{D_S \phi_r} \left(\frac{X_{mr}}{X_{mr} + X_{ms}} \right) \tag{16}$$

Ball consumption is defined as:

$$BC = \frac{P_{mill}\varphi}{\phi_b} \left(\frac{X_{mb}}{D_S (X_{mr} + X_{ms}) + D_B X_{mb}} \right) \tag{17}$$

The fines produced from the ground ore is defined as:

$$FP = P_{mill} \left(D_S \phi_f \left[1 + \alpha_{\phi_f} \left(LOAD/v_{mill} - v_{P_{max}} \right) \right] \right)^{-1} \tag{18}$$

3.3 Mixed-sump Module

For mixed-sump module it is assumed that the constituents inside the sump are fully mixed. The only constituents (states) found in this module are water, solids and fines. The population volume balance of the hold-up of water (X_{sw}), solids (X_{ss}) and fines (X_{sf}) in the sump are defined as:

$$\dot{X}_{sw} = V_{mwo} - V_{swo} + SFW \tag{19}$$

$$\dot{X}_{ss} = V_{mso} - V_{sso} \tag{20}$$

$$\dot{X}_{sf} = V_{mfo} - V_{sfo} \tag{21}$$

Equation (19) includes the flow-rate of water added to the slurry in the sump (SFW) to manipulate the density of the slurry feed to the classifier. The classifier feed density has a significant impact on the performance of the classifier:

$$CFD = (X_{sw} + D_s X_{ss}) / (X_{sw} + X_{ss}) \tag{22}$$

The sump discharge flow-rates of water (V_{swo}), solids (V_{swo}) and fines (V_{sfo}) are defined as:

$$V_{swo} = CFF\,(X_{sw}/SVOL) \tag{23}$$

$$V_{sso} = CFF\,(X_{ss}/SVOL) \tag{24}$$

$$V_{sfo} = CFF\,(X_{sf}/SVOL) \tag{25}$$

where the volume of the sump filled is given by:

$$SVOL = X_{sw} + X_{ss} \tag{26}$$

3.4 Classification Screen Module

Because the dynamics of the screen is much faster than the rest of the circuit, the screen is described by a set of algebraic equations. The sizing performance of screens can be presented by an efficiency curve which describes the proportion of a given size of solids reporting to the oversize product. The efficiency curve for the undersize flow will be the complement of the oversize flow efficiency curve (Napier-Munn et al., 1999).

Water, fines and a fraction of the solids pass through the apertures of the screen to the undersize flow. The oversize flow consists only of the fraction of the solids too large to pass through the screen apertures. It is assumed that a negligible amount of water pass to the oversize flow. Therefore, the flow-rates at the oversize of the screen are:

$$V_{csos} = D_1 V_{csi} \tag{27}$$

$$V_{cwos} = V_{cfos} = 0 \tag{28}$$

where D_1 is the proportion of the ore within the solids size class which report to the oversize product. The flow-rates at the undersize of the screen are defined as:

$$V_{cwus} = CWA + V_{swo} \tag{29}$$

$$V_{csus} = (1 - D_1) V_{sso} \tag{30}$$

$$V_{cfus} = V_{sfo} \tag{31}$$

The final product particle size estimate is given by:

$$PSE = 100\,(D_2 - V_{cfus}/V_{csus}) \tag{32}$$

where D_2 is a fitting parameter.

4. STATE AND PARAMETER ESTIMATION

Dynamic data of the grinding mill circuit was obtained from a real plant. The data represent the operation of the circuit during a step-test campaign by the operators of the plant to determine linear transfer function models of the circuit. Because of the limitations of linear transfer function models, this study aims to fit the non-linear model described in Section 3 to the plant. This should provide a more detailed model of the plant for control purposes without increasing modelling costs.

The following input u and output y variables were measured by the plant:

$$u = [MIW\ MFS\ MFB\ SFW\ CFF]^T \tag{33}$$

$$y = [P_{mill}\ SVOL\ CFD\ PSE]^T \tag{34}$$

All the states in the mill and sump cannot be measured directly and need to be estimated:

$$x = [X_{mw}\ X_{ms}\ X_{mf}\ X_{mr}\ X_{mb}\ X_{sw}\ X_{ss}\ X_{sf}]^T \tag{35}$$

Although many of the parameters in the model can be obtained directly from plant data, the following parameters need to be estimated:

$$p = [\delta_{P_s}\ \delta_{P_v}\ D_1\ D_2\ \phi_b\ \phi_r\ V_V\ \chi_P]^T \tag{36}$$

The unmeasurable states and parameters within the mill and the sump can be estimated by an EKF by creating an augmented states vector $z = [x \ \ p]^T$.

The description of the EKF below is taken from Simon (2006). The process considered in this study is governed by continuous-time dynamics and discrete time measurements:

$$\dot{z} = f(z, u, w, t) \\ y_k = h_k(z_k, u_k, v_k) \\ w(t) \sim (0, Q)\ ;\ v_k \sim (0, R_k) \tag{37}$$

The process noise $w(t)$ is continuous-time white noise with covariance Q and the measurement noise v_k is discrete-time white noise with covariance R_k. Between each measurement, the state estimate $\hat{z}$ and its covariance P is propagated according to the known non-linear dynamics of the system:

$$\dot{\hat{z}} = f(\hat{z}, u, 0, t) \\ \dot{P} = AP + PA^T + Q \tag{38}$$

where $A = \frac{\delta f}{\delta z} \mid_{\hat{z}}$ and it is assumed that $\frac{\delta f}{\delta w} \mid_{\hat{z}} = I$. Equation (38) propagates $\hat{z}$ from $\hat{z}_{k-1}^{+}$ to $\hat{z}_{k}^{-}$ and propagates P from P_{k-1}^{+} to P_{k}^{-}. At each time measurement the state estimate and its covariance are updated:

$$\begin{aligned} K_k &= P_k^- H_k^T \left(H_k P_k^- H_k^T + R_k\right)^{-1} \\ \hat{z}_k^+ &= \hat{z}_k^- + K_k \left[y_k - h_k\left(\hat{z}_k^-, u, v_0, t_k\right)\right] \\ P_k^+ &= \left(I - K_k H_k\right) P_k^- \left(I - K_k H_k\right)^T + K_k R_k K_k^T \end{aligned} \tag{39}$$

where $H_k = \frac{\delta h}{\delta z} \mid_{\hat{z}_k^-}$ and it is assumed that $\frac{\delta h}{\delta v} \mid_{\hat{z}} = I$.

Equations (40)-(48) below describe function f of eq. (37). It is assumed that the additional states p in the augmented state vector z have no dynamics. Note that the flow-rate V_{sso} in eq. (41) is delayed by $T_{sc} + T_{cm}$, the time delays between the sump and classifier and between the classifier and mill respectively.

$$\dot{X}_{mw} = MIW - V_V \varphi X_{mw} X_{mw} / \left(X_{ms} + X_{mw}\right) \tag{40}$$

$$\begin{aligned} \dot{X}_{ms} = \tfrac{MFS}{D_S}\left(1 - \alpha_r\right) - \tfrac{V_V \varphi X_{mw} X_{ms}}{X_{ms} + X_{mw}} + \\ \tfrac{P_{mill}\varphi}{D_S \phi_r}\left(\tfrac{X_{mr}}{X_{mr} + X_{ms}}\right) + D_1 V_{sso} \end{aligned} \tag{41}$$

$$\begin{aligned} \dot{X}_{mf} = \tfrac{MFS}{D_S}\alpha_f - V_V \varphi X_{mw} X_{mf} / \left(X_{ms} + X_{mw}\right) + \\ \tfrac{P_{mill}}{D_S \phi_f}\left[1 + \alpha_{\phi_f}\left(\tfrac{X_{mw} + X_{mr} + X_{ms} + X_{mb}}{v_{mill}} - v_{P_{max}}\right)\right]^{-1} \end{aligned} \tag{42}$$

$$\dot{X}_{mr} = \frac{MFS}{D_S}\alpha_r - \frac{P_{mill}\varphi}{D_S \phi_r}\left(\frac{X_{mr}}{X_{mr} + X_{ms}}\right) \tag{43}$$

$$\dot{X}_{mb} = \frac{MFB}{D_B} - \frac{P_{mill}\varphi X_{mb}}{\phi_b\left[D_S\left(X_{mr} + X_{ms}\right) + D_B X_{mb}\right]} \tag{44}$$

$$\dot{X}_{sw} = \frac{V_V \varphi X_{mw} X_{mw}}{X_{ms} + X_{mw}} - \frac{CFF X_{sw}}{X_{sw} + X_{ss}} + SFW \tag{45}$$

$$\dot{X}_{ss} = \frac{V_V \varphi X_{mw} X_{ms}}{X_{ms} + X_{mw}} - \frac{CFF X_{ss}}{X_{sw} + X_{ss}} \tag{46}$$

$$\dot{X}_{sf} = \frac{V_V \varphi X_{mw} X_{mf}}{X_{ms} + X_{mw}} - \frac{CFF X_{sf}}{X_{sw} + X_{ss}} \tag{47}$$

$$\dot{\delta}_{P_s} = \dot{\delta}_{P_v} = \dot{D}_1 = \dot{D}_2 = \dot{\phi}_b = \dot{\phi}_r = \dot{V}_V = \dot{\chi}_P = 0 \tag{48}$$

Function h in eq. (37) can be constructed from eqs. (14), (26), (22) and (32). Because real plant data was used, it was necessary to reject outliers in the output data. At each sampling instance t_k the vector of measured output data y_k is presented to the EKF. If the vector contains an outlier, the state estimate $\hat{z}_k^-$ and its covariance P_k^- are not updated according to eq. (39), but simply propagated further based on the previous measurements at t_{k-1}. Because the measurement noise matrix for the data from the plant was estimated as $R = \mathrm{diag}\left[400,\ 20,\ 0.1,\ 5\right]^2$, outliers in the data were rejected if the difference between the actual data and the model output was greater than one standard deviation of the diagonal elements in the noise matrix $\left|y_k - h_k\left(\hat{z}_k^-, u, v_0, t_k\right)\right| \geq \left[400\ 20\ 0.1\ 5\right]^T$.

5. RESULTS AND DISCUSSION

Although spillage water added to the sump did not form part of the model formulation in the previous section, the plant analysed in this study added significant spillage water to the sump. The added water has a significant impact on both $SVOL$ and CFD. To account for the effect of spillage water, another state to be estimated was added to vector z:

$$z' = \left[z \quad z_{17}\right]^T \tag{49}$$

This required a change to function f in eq. (45):

$$\dot{X}_{sw} = \frac{V_V \varphi X_{mw} X_{mw}}{X_{ms} + X_{mw}} - \frac{CFF X_{sw}}{X_{sw} + X_{ss}} + SFW + z_{17} \tag{50}$$

and the addition of a new equation to function f:

$$\dot{z}_{17} = 0 \tag{51}$$

The initialization values of the state estimate z', its covariance P as well as the covariance of the process noise matrix Q are shown in Table 4. These values were obtained from an analysis of dynamic data of the plant at steady-state. The values for the remaining parameters calculable from plant data are shown in Table 5.

The output of the circuit determined from the states and parameters estimated by the EKF and the actual output of the system as measured during the step-test campaign of the plant can be seen in Figs. 2 and 3. The four controlled variables, P_{mill}, $SVOL$, CFD and PSE follow the measured data of the plant closely.

The mill and sump states of vector x in eq. (35) as estimated by the EKF are shown in Fig. 4. The parameters in vector p of eq. (36) as estimated by the EKF are shown in Figs. 5 and 6. Fig. 7 shows the estimation of the spillage water added to the sump.

The sudden change of V_V in Fig. 6b at approximately 7.5 h can be attributed to a sudden change in the operating condition of the plant. The change in the operating condition can be seen in the change of the controlled variables in Figs. 2 and 3 at 7.5 h.

It is necessary to test the effectiveness of the EKF estimation by means of a consistency check. This requires the calculation of $\tilde{z} = z - \hat{z}$ where $\tilde{z}$ is the error between the EKF estimation $\hat{z}$ and the actual state value z. However, the consistency check cannot be done because the actual state vector z was not measured by the plant during the step-tests. This vector can rarely be measured. Still, the EKF should be tuned so that the standard deviation of each state estimate $(P_k^+)^{0.5}$ converge. The standard deviation of each state estimate was normalised with the respective state value in $\sqrt{P_0}$ and is shown in Figs. 8-10. In all cases the standard deviation of the state estimate is converging, which is a fair indication of proper tuning of the EKF.

The system described in eq. (37) was considered to be state observable if for any time $t_1 > 0$ the initial state z'_0 can be determined from the time history of the input u and the output y in the time interval $[0, t_1]$. The observability was tested by considering the modes m_i of $A = \delta f / \delta z'$ which are observable if and only if $\frac{\delta h}{\delta z'} t_i \neq 0$ for all right eigenvectors t_i associated with m_i. The system is observable if and only if every mode m_i is observable (Skogestad and Postlethwaite, 2005). It was found that the states in vector z' are observable for the estimation period. This method was deemed valid since the EKF linearises functions f and h_k in eq. (37) as shown in eq. (39).

According to Fig. 11 which shows the autocorrelation of $y_k - h_k(z_k^-, u_k, v_0, t_k)$, the assumption of white noise for P_{mill}, $SVOL$, CFD and PSE is valid.

Although results show that the EKF gives fair results, the covariance for some parameters does not readily converge

Table 4. Initial values for states estimate ($\hat{z}_0$), state standard deviations ($\sqrt{P_0}$) and noise standard deviations ($\sqrt{Q}$)

Z'	Z'_0	$\sqrt{P_0}$	$\sqrt{Q}$	Z'	Z'_0	$\sqrt{P_0}$	$\sqrt{Q}$
X_{mw}	31.22	20	5	δ_{P_s}	3	10	1
X_{ms}	37.64	20	10	D_1	0.15	0.1	0.0025
X_{mf}	12.96	5	5	D_2	0.75	0.2	0.1
X_{mr}	21.34	15	10	ϕ_b	4028	500	5
X_{mb}	38.69	10	1	ϕ_r	2.12	0.5	0.03
X_{sw}	49.72	15	5	V_V	15.60	10	6
X_{ss}	13.28	5	2	χ_P	-2	10	1
X_{sf}	4.57	2.5	0.5	z_{17}	80	40	40
δ_{P_v}	-3.5	10	1				

Table 5. Model parameter values

Parm	Value	Parm	Value	Parm	Value
α_f	0.01	α_r	0.8	α_{ϕ_f}	0.01
α_P	1	α_{speed}	0.75	D_S	3.6 t/m^3
D_B	7.85 t/m^3	ε_{sv}	0.6	ϕ_f	40.2 kWh/t
$\varphi_{P_{max}}$	0.42	P_{max}	7440kW	v_{mill}	379 m^3
$v_{P_{max}}$	0.34	T_{sc}	30 s	T_{cm}	10 s

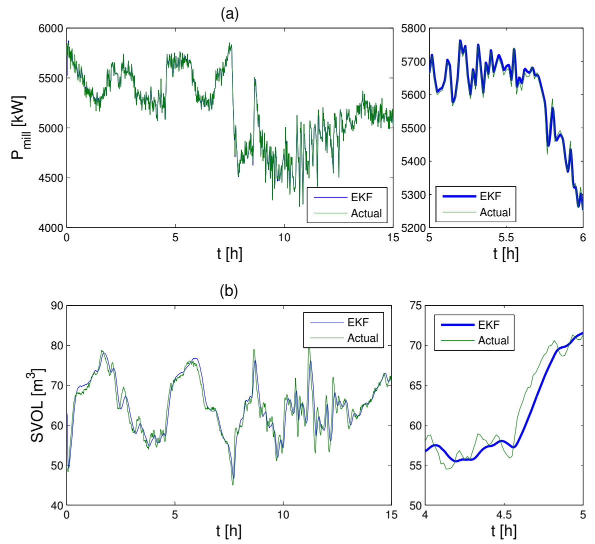

Fig. 2. (a) Actual P_{mill} versus P_{mill} estimated from EKF output (normal and zoomed plot). (b) Actual $SVOL$ versus $SVOL$ estimated from EKF output (normal and zoomed plot).

to zero. An unscented Kalman or particle filter may improve the convergence rate and thus the confidence in the parameter estimations.

6. CONCLUSION

The unknown parameters and states for a grinding mill circuit model for process control was estimated by an EKF from real plant data. The output of the circuit as predicted by the model from the estimated states and parameters closely follow the actual output measured by the plant. The estimation of the parameters and states as the process continuous makes it possible to continuously update process models. This estimation process may be used to reduce model-plant mismatch for models used in model predictive controllers and could improve overall controller performance.

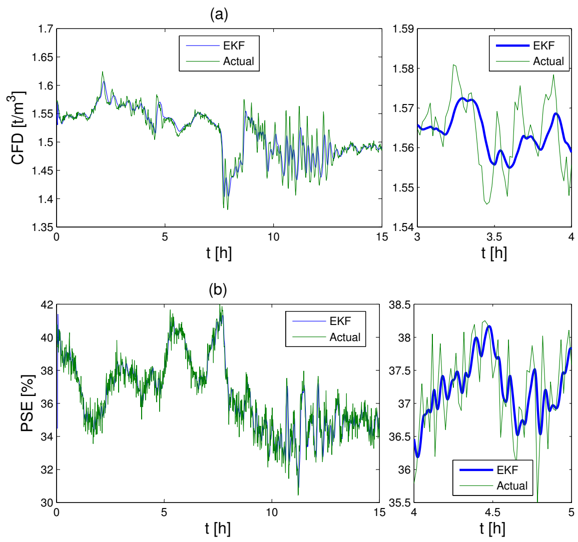

Fig. 3. (a) Actual CFD versus CFD estimated from EKF output (normal and zoomed plot). (b) Actual PSE versus PSE estimated from EKF output (normal and zoomed plot).

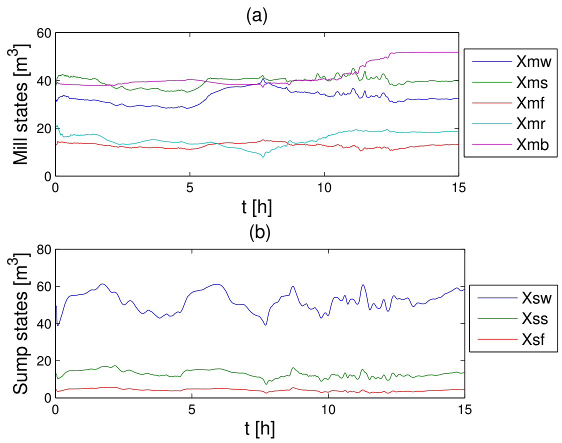

Fig. 4. (a) EKF estimates for mill states. (b) EKF estimates for sump states.

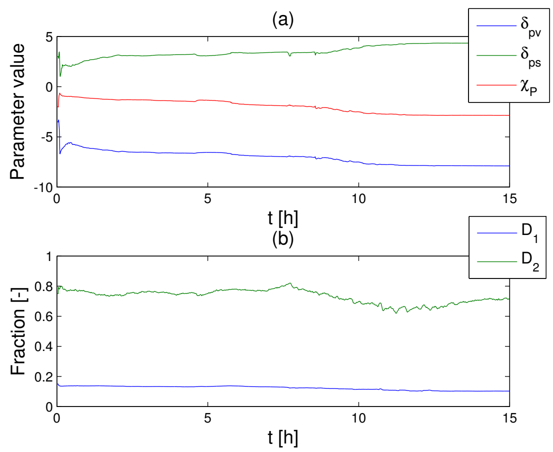

Fig. 5. (a) EKF estimates for δ_{P_v}, δ_{P_s} and χ_P (b) EKF estimates for D_1 and D_2.

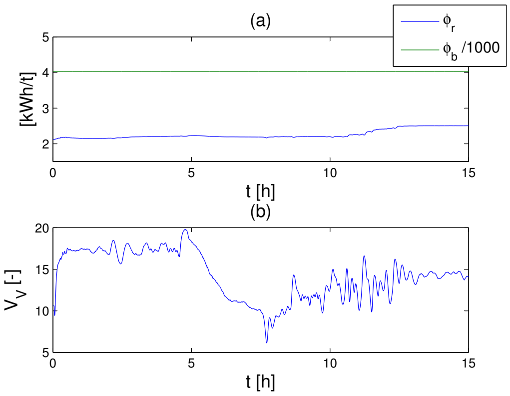

Fig. 6. (a) EKF estimates for ϕ_r and $\frac{\phi_b}{1000}$ (b) EKF estimate for V_V.

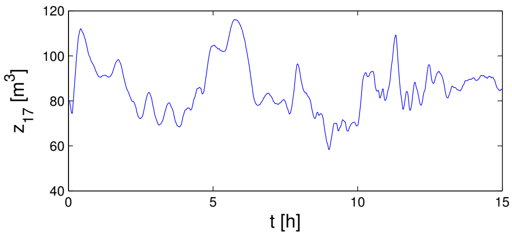

Fig. 7. EKF estimate for z_{17}.

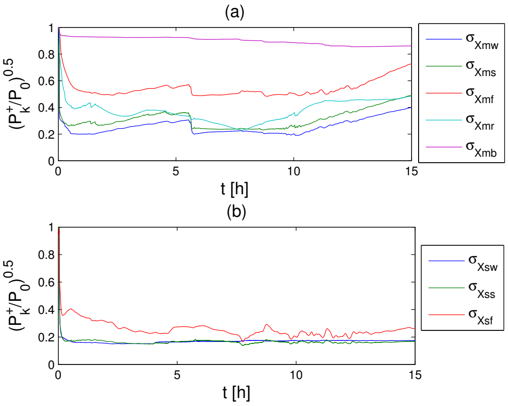

Fig. 8. $(P_k^+/P_0)^{0.5}$ for (a) mill states and (b) sump states.

REFERENCES

Chen, X., Zhai, J., Li, S., and Li, Q. (2007). Application of model predictive control in ball mill grinding circuit. *Minerals Eng.*, 20(11), 1099 – 1108.

Coetzee, L.C., Craig, I.K., and Kerrigan, E.C. (2010). Robust nonlinear model predictive control of a run-of-mine ore milling circuit. *IEEE Trans. Control Syst. Technol.*, 18(1), 222–229.

le Roux, J.D., Craig, I.K., Hulbert, D.G., and Hinde, A.L. (2013). Analysis and validation of a run-of-mine ore grinding mill circuit model for process control. *Minerals Eng.*, 43-44, 121–134.

Napier-Munn, T.J., Morrell, S., Morrison, R.D., and Kojovic, T. (1999). *Mineral Communition Circuits: Their Operation and Optimisation*. JKMRC Monograph Series in Mining and Mineral Processing, 2nd edition, 154–191.

Olivier, L., Huang, B., and Craig, I. (2012). Dual particle filters for state and parameter estimation with application to a run-of-mine ore mill. *J. Process Control*, 22(4), 710–717.

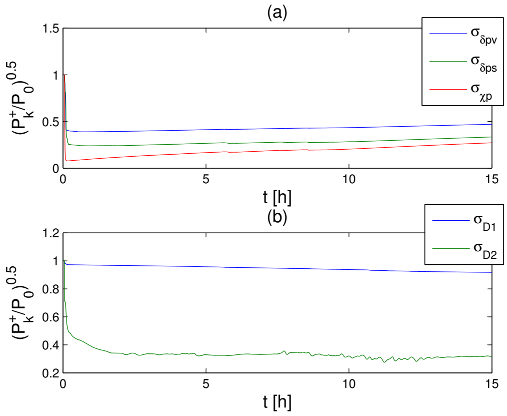

Fig. 9. $(P_k^+/P_0)^{0.5}$ for (a) mill power draw parameters and (b) screen parameters.

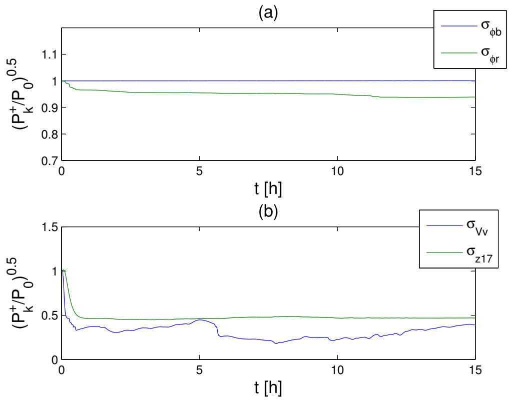

Fig. 10. $(P_k^+/P_0)^{0.5}$ for (a) breakage parameters and (b) V_V and z_{17}.

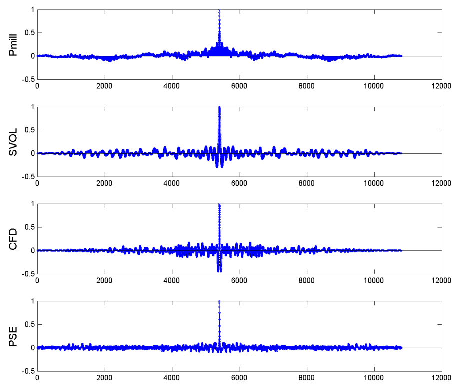

Fig. 11. Autocorrelation of error signal in eq. (37): $y_{error} = y_k - h_k(z_k^-, u_k, v_0, t_k)$

Simon, D.J. (2006). *Optimal State Estimation*. John Wiley and Sons, Inc., 1st edition, 395–409.

Skogestad, S. and Postlethwaite, I. (2005). *Multivariable Feedback Control: Analysis and Design*. John Wiley and Sons, Inc., 2nd edition, 127–134.